

# Eigenmodes of triaxial ellipsoidal acoustical cavities with mixed boundary conditions

M. Willatzen<sup>a)</sup>

Mads Clausen Institute for Product Innovation, University of Southern Denmark, Grundtvigs Alle 150, DK-6400 Sønderborg, Denmark

L. C. Lew Yan Voon<sup>b)</sup>

Department of Physics, Worcester Polytechnic Institute, 100 Institute Road, Worcester, Massachusetts 01609

(Received 19 December 2003; revised 27 September 2004; accepted 27 September 2004)

The linear acoustics problem of resonant vibrational modes in a triaxial ellipsoidal acoustic cavity with walls of arbitrary acoustic impedance has been quasi-analytically solved using the Frobenius power-series expansion method. Eigenmode results are presented for the lowest two eigenmodes in cases with pressure-release, rigid-wall, and lossy-wall boundary conditions. A mode crossing is obtained as a function of the specific acoustic impedance of the wall; the degeneracy is not symmetry related. Furthermore, the damping of the wave is found to be maximal near the crossing. © 2004 Acoustical Society of America. [DOI: 10.1121/1.1819391]

PACS numbers: 43.20.Ks [MO]

Pages: 3279–3283

## I. INTRODUCTION

The knowledge of analytical acoustic cavity eigenmodes is still important in spite of advances in computational acoustics.<sup>1</sup> Indeed, there remains computational difficulties in obtaining the eigenmodes of irregular three-dimensional cavities using techniques such as the boundary-element method.<sup>2</sup> Nevertheless, the normal modes are known to be analytically obtainable in cavities of various shapes, describable in terms of eleven orthogonal curvilinear coordinate systems.<sup>3</sup> The solutions for rectangular, cylindrical, and spherical cavities are now textbook examples.<sup>4</sup> Other shapes that have been solved exactly are the spheroid,<sup>5</sup> the elliptic cylinder,<sup>6</sup> the parabolic cylinder,<sup>7</sup> and the parabolic rotational lens.<sup>8</sup> Yet, the most general cavity with a one-coordinate surface, the triaxial ellipsoid, has not been solved. Nevertheless, physical models in acoustics using the latter shape abound including, for example, for the study of ocean acoustics,<sup>9</sup> of cavitation in bubbles,<sup>10</sup> and of the human body;<sup>11</sup> these works have mostly dealt with scattering problems. Indeed, the approximation of an irregular body by an ellipsoid (the so-called Brillouin ellipsoid<sup>12</sup>) is common. We also note that previous work on analytic shapes in acoustics were often only done for rigid-wall and pressure-release boundary conditions. One exception is the discussion in Morse and Ingard<sup>13</sup> for rectangular rooms.

The ellipsoidal cavity is fundamentally important since it can be viewed as the limit of a highly distorted spherical cavity and exact results will still hold even when perturbation theory on the sphere is no longer valid. The lowered symmetry compared to a sphere and a spheroid makes it ideal as an analytical model of a nonsymmetric cavity. In addition, the one-parameter nature of the bounding surface

also allows a straightforward implementation of a uniform boundary condition. Finally, the cavity might have acoustical characteristics that are more desirable than either the spherical or the spheroidal cavity since the mode degeneracies present in the latter are expected to be completely removed due to the lower shape symmetry.

In this Letter, we present the solution to the triaxial ellipsoidal cavity problem analytically in terms of Lamé wave functions. The construction of the latter functions can be carried out independently of the boundary condition. This allows an efficient computation of the complex eigenfrequencies for walls with arbitrary acoustic impedance.

## II. THEORY

The mathematical formulation of the problem is finding the discrete spectrum of the Helmholtz equation,<sup>14</sup>

$$\nabla^2 P(\mathbf{r}) + k^2 P(\mathbf{r}) = 0, \quad (1)$$

subject to the mixed boundary condition on the surface of the ellipsoidal cavity:

$$\eta \frac{\partial P}{\partial n} + ikP = 0, \quad (2)$$

where  $P(\mathbf{r})$  is the acoustic pressure field,  $k$  the wave number, and  $\eta$  is the specific impedance. The latter is given by  $Z/(\rho_0 c_0)$  where  $Z$  is the wall acoustic impedance,  $c_0$  is the speed of sound, and  $\rho_0$  the background or equilibrium medium mass density. In order to reduce the number of degrees of freedom in the problem, we will only consider the case where the acoustic impedance is real and frequency independent, and the surface is locally reactive.<sup>13</sup> Nevertheless, the general boundary condition, Eq. (2), is still complex and frequency dependent.

<sup>a)</sup>Electronic mail: willatzen@mci.sdu.dk; phone: +45 65 50 16 82; fax: +45 65 50 16 60.

<sup>b)</sup>Electronic mail: llew@wpi.edu; phone +1 508 831 5249; fax: +1 508 831 5886.

## A. Ellipsoidal coordinates and the triaxial ellipsoid

Ellipsoidal coordinates (EC) are defined by three families of orthogonal confocal quadric surfaces. The latter are defined by the equation

$$\frac{x^2}{\xi^2 - a^2} + \frac{y^2}{\xi^2 - b^2} + \frac{z^2}{\xi^2} = 1, \quad a \geq b \geq 0, \quad (3)$$

where different types of surfaces are obtained for different values of the parameter  $\xi$ . Those three types of surfaces are obtained as follows.<sup>3</sup> If  $\xi \equiv \xi_1 > a$ , all three terms on the left hand side of Eq. (3) are positive and the equation describes an ellipsoidal surface. If  $a > \xi \equiv \xi_2 > b$ , the first term on the left hand side of Eq. (3) is negative; the quadric surfaces are then a family of confocal hyperboloids of one sheet. If  $b > \xi \equiv \xi_3 > 0$ , the first two terms on the left hand side of Eq. (3) are negative; the quadric surfaces are confocal hyperboloids of two sheets.

The relationship of the EC  $\xi_1, \xi_2, \xi_3$  to the Cartesian ones is<sup>3,15,16</sup>

$$x = \frac{(\xi_1^2 - a^2)^{1/2}(\xi_2^2 - a^2)^{1/2}(\xi_3^2 - a^2)^{1/2}}{a(a^2 - b^2)^{1/2}}, \quad (4)$$

$$y = \frac{(\xi_1^2 - b^2)^{1/2}(\xi_2^2 - b^2)^{1/2}(\xi_3^2 - b^2)^{1/2}}{b(b^2 - a^2)^{1/2}}, \quad z = \frac{\xi_1 \xi_2 \xi_3}{ab},$$

with

$$\xi_1 > a > \xi_2 > b > \xi_3 > 0. \quad (5)$$

One set of  $\xi_1, \xi_2, \xi_3$  corresponds to eight Cartesian points.

In general,  $a$  and  $b$  can take on any values subject to the convention given in Eq. (5). It turns out the values are fixed when space is partitioned by an ellipsoid. Thus, let the Cartesian coordinates of the points of intersection of the ellipsoid with the Cartesian axes be  $\pm x_0, \pm y_0, \pm z_0$ . Then, Eq. (3) for  $\xi = \xi_1$  relates  $x_0, y_0, z_0$  to  $a, b$ :

$$\xi_{1ref} = z_0, \quad (6)$$

$$a = (\xi_{1ref}^2 - x_0^2)^{1/2}, \quad (7)$$

$$b = (\xi_{1ref}^2 - y_0^2)^{1/2}, \quad (8)$$

where  $\xi_{1ref}$  is the value of  $\xi_1$  on the ellipsoidal surface (recall that  $\xi_1$  alone defines an ellipsoidal surface). We observe that the ordering  $a > b > 0$  implies  $z_0 > y_0 > x_0$ .

## B. Separation of variables in ellipsoidal coordinates

The above problem [Eqs. (1)–(2)] is separable in EC. Let

$$\Psi = X_1(\xi_1)X_2(\xi_2)X_3(\xi_3). \quad (9)$$

The insertion of Eq. (9) in Eq. (1) leads to three ordinary differential equations in the separated functions  $X_i$ :

$$\sqrt{(\xi_1^2 - a^2)(\xi_1^2 - b^2)} \frac{d}{d\xi_1} \left[ \sqrt{(\xi_1^2 - a^2)(\xi_1^2 - b^2)} \frac{dX_1}{d\xi_1} \right]$$

$$= (-k^2 \xi_1^4 + \alpha_2 \xi_1^2 - \kappa) X_1,$$

$$\sqrt{(a^2 - \xi_2^2)(\xi_2^2 - b^2)} \frac{d}{d\xi_2} \left[ \sqrt{(a^2 - \xi_2^2)(\xi_2^2 - b^2)} \frac{dX_2}{d\xi_2} \right]$$

$$= -(-k^2 \xi_2^4 + \alpha_2 \xi_2^2 - \kappa) X_2, \quad (10)$$

$$\sqrt{(a^2 - \xi_3^2)(b^2 - \xi_3^2)} \frac{d}{d\xi_3} \left[ \sqrt{(a^2 - \xi_3^2)(b^2 - \xi_3^2)} \frac{dX_3}{d\xi_3} \right]$$

$$= (-k^2 \xi_3^4 + \alpha_2 \xi_3^2 - \kappa) X_3,$$

The constants  $\alpha_2$  and  $\kappa$  are separation constants determined by the boundary conditions and the fact that any acceptable solution is finite and differentiable within the ellipsoidal enclosure. Equations (10) can be rewritten as ( $i = 1, 2, 3$ )

$$(\xi_i^2 - a^2)(\xi_i^2 - b^2) \frac{d^2 X_i}{d\xi_i^2} + \xi_i [2\xi_i^2 - (a^2 + b^2)] \frac{dX_i}{d\xi_i}$$

$$+ [k^2 \xi_i^4 - \alpha_2 \xi_i^2 + \kappa] X_i = 0, \quad (11)$$

an equation known as the ellipsoidal or Lamé wave equation.<sup>3</sup> By making the transformation,

$$t_i = \frac{\xi_i^2}{b^2}, \quad (12)$$

we obtain the form due to Arscott *et al.*<sup>17</sup>

$$t_i(t_i - 1)(t_i - c) \frac{d^2 X_i}{dt_i^2} + \frac{1}{2} [3t_i^2 - 2(1 + c)t_i + c] \frac{dX_i}{dt_i}$$

$$+ [\lambda + \mu t_i + \gamma t_i^2] X_i = 0, \quad (13)$$

where

$$\frac{a^2}{b^2} = c, \quad \kappa = 4b^2\lambda, \quad \alpha_2 = -4\mu, \quad k^2 = \frac{4}{b^2} \gamma. \quad (14)$$

It is always possible to write  $X_i$  in the general form<sup>17</sup>

$$X_i(t_i) = t_i^{\rho/2} (t_i - 1)^{\sigma/2} (t_i - c)^{\tau/2} F(t_i), \quad (15)$$

where  $\rho, \sigma$ , and  $\tau$  are either 0 or 1, i.e., eight different types of  $X_i$  are possible. The function  $F$  must be found using a quasi-analytical approach. Inserting Eq. (15) into Eq. (13) leads to the differential equation<sup>17</sup>

$$t_i(t_i - 1)(t_i - c) \frac{d^2 F_i}{dt_i^2} + \frac{1}{2} (A_2 t_i^2 - 2A_1 t_i + A_0) \frac{dF_i}{dt_i}$$

$$+ (\lambda - \lambda_0 + (\mu + \mu_0)t_i + \gamma t_i^2) F_i = 0, \quad (16)$$

where

$$\lambda_0 = \frac{1}{4} [(\rho + \tau)^2 + (\rho + \sigma)^2 c],$$

$$\mu_0 = \frac{1}{4} (\rho + \sigma + \tau)(\rho + \sigma + \tau + 1), \quad A_0 = (2\rho + 1)c, \quad (17)$$

$$A_1 = (1 + \rho)(1 + c) + \tau + \sigma c, \quad A_2 = 2(\rho + \sigma + \tau) + 3.$$

Equation (16) can be solved formally by using the Frobenius power-series expansion method,<sup>8</sup> i.e.,

$$F_i(t_i) = \sum_{r=0}^{\infty} a_r (t_i - t_0)^r, \quad (18)$$

where  $t_0$  is an expansion parameter. The insertion of Eq. (18) into Eq. (16) leads to a five-term recursion formula in the coefficients  $a_r$ . First, solutions are found for  $\gamma=0$  (the Lamé equation). Solutions exist whenever

$$\mu = -\mu_0 - n(n-1) - \frac{1}{2}A_2n, \quad (19)$$

where  $n$  is an integer  $(0,1,2,\dots)$ . The possible values of  $\lambda$  are then found by solving an  $n+1$ -polynomial equation in  $\lambda$ , i.e.,  $n+1$  real  $\lambda$  solutions exist for each  $n$  ( $\lambda=\lambda_{nm}; m=0,1,2,\dots,n$ ).<sup>17</sup> These solutions give initial values at  $\gamma=0$  for the subsequent computation of separation constants  $\mu(\gamma)$  and  $\lambda(\gamma)$  at finite  $\gamma$  values. Values of  $\mu(\gamma)$  and  $\lambda(\gamma)$  are obtained next using Newton's method which is known to be locally convergent when employing sufficiently small steps in  $\gamma$ . In the present work,  $\Delta\gamma$  is chosen to be 0.01 starting from  $\gamma=0$  and  $t_0$  is chosen to be 1 for all the eight cases:  $\rho, \sigma, \tau$  equal to 0 or 1.

Once a set of solution parameters  $\gamma, \mu$ , and  $\lambda$  has been obtained, the total eigenfunction within one octant of the ellipsoid becomes

$$\Psi(\xi_1, \xi_2, \xi_3) = X(\xi_1)X(\xi_2)X(\xi_3), \quad (20)$$

where  $X$  satisfies the ellipsoidal wave equation [Eq. (11)]. A second solution  $Y$  to Eq. (11) exists, however,  $\nabla Y$  is not well-defined everywhere inside the ellipsoid and  $Y$  can thus be disregarded as a possible solution. For example,  $\nabla Y$  diverges as  $\xi_1 \rightarrow a+$ ,  $\xi_2 \rightarrow a-$ , and  $\xi_3 \rightarrow 0+$ .

### III. NUMERICAL RESULTS AND DISCUSSIONS

Having determined the characteristic values (i.e.,  $\mu$  and  $\lambda$  versus  $\gamma$ ), we impose the boundary condition [Eq. (2)] so as to obtain a discrete set of solutions for the separable constants:  $(\gamma_i, \mu_i, \lambda_i)$  where  $i=1,2,3,4,\dots$ , for each of the eight cases:  $\rho=\pm 1, \sigma=\pm 1, \tau=\pm 1$ . Once these separation constants are determined, eigenfrequencies and associated eigenfunctions (pressure modes) are easily specified as will be described next. The following relations apply [refer to Eq. (14)]:

$$k_i = \frac{2\sqrt{\gamma_i}}{b}, \quad f_i = \frac{\omega_i}{2\pi} = \frac{k_i c_0}{2\pi} = \frac{\sqrt{\gamma_i} c_0}{\pi b}, \quad (21)$$

where  $k_i$ ,  $\omega_i$ , and  $f_i$  are the wavenumber, angular frequency, and the frequency of pressure mode  $i$ , respectively. For finite values of  $\eta$ , the separation constants are complex; then, both the eigenvalues and eigenfunctions are also complex. In the following, we consider an ellipsoidal acoustical enclosure with absolute semiaxes  $(x_0, y_0, z_0) = (1.0, 1.5, 2.0)$  m associated with the parameter values:  $\xi_{1ref} = 2.0$  m,  $a = 1.732$  m,  $b = 1.323$  m, and  $c = a^2/b^2 = 1.714$ .

#### A. Modes in a triaxial ellipsoid with pressure-release walls

In this subsection, it is assumed that the ellipsoidal cavity walls are characterized by a specific impedance equal to zero, i.e.,  $\eta=0$  corresponding to pressure-release boundary conditions. The general boundary condition then degenerates into a Dirichlet boundary condition:

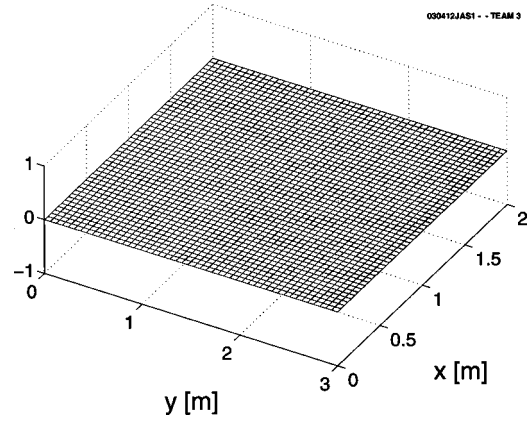


FIG. 1. The fundamental and first-excited modes plotted along three orthogonal planes (from left to right:  $xy$ ,  $yz$ ,  $xz$ ). They correspond pairwise to pressure-release (i.e., first two rows), rigid-wall (middle two rows), and lossy-wall (with specific impedance  $\eta=0.6$ ) boundary conditions. For the latter case, the plots shown are the modulus of the complex eigenmode.

$$\Psi|_{(\xi_1=\xi_{1ref})} = 0. \quad (22)$$

The fundamental mode with  $\gamma=2.41$ ,  $\rho=\sigma=\tau=0$  is shown as a function of  $x, y$  in the  $z=0$  plane (left plot),  $x, z$  in the  $y=0$  plane (middle plot), and  $y, z$  in the  $x=0$  plane (right plot) in the first row of Fig. 1. The corresponding eigenfrequency is 128 Hz for a cavity containing air at room temperature (with a sound speed of  $c_0=343$  m/s). Note that the fundamental-mode frequency for a spherical enclosure of the same volume is 119 Hz (in agreement with the intuitive rule that the fundamental mode frequency corresponding to Dirichlet boundary conditions must increase with increasing spatial asymmetry at a constant volume). It is evident that this state has no nodes along the three planes and peaks at the center of the ellipsoid similar to what is found for the groundstate of a spherical cavity. It is important to realize that since this mode is obtained as an exact series solution, it is smooth and differentiable. This contrasts to solutions obtained via purely numerical techniques such as finite difference and finite element methods that only give the eigenmodes at the grid or nodal points and, due to the severe memory requirements of a three-dimensional problem, are often not very smooth.

In the second row of Fig. 1, similar plots are shown for the first excited state along the three planes. The associated eigenfrequency is 161 Hz ( $\gamma=3.79$ ) and indices  $\rho, \sigma, \tau$  are 1, 0, 0, respectively. As one observes, the eigenmode is zero in the  $z=0$  plane because  $\xi_3=0$  when  $z=0$ , and

$$\Psi(\xi_1, \xi_2, \xi_3) = \frac{\xi_1 \xi_2 \xi_3}{b^3} F(\xi_1)F(\xi_2)F(\xi_3), \quad (23)$$

where  $F$  is the solution to Eq. (16) (note that  $t=\xi_i^2/b^2$ ). However,  $\Psi$  is nonzero when plotted in the  $y=0$  and  $x=0$  planes corresponding to  $\xi_2=b>0$  (or  $\xi_3=b>0$ ) and  $\xi_1=a>0$  (or  $\xi_2=a>0$ ), respectively. Observe also that the eigenmode is nodeless in both planes. This solution resembles the first excited state for the sphere in having a nodal plane. However, all solutions are found to be nondegenerate in contrast to the spherical case. For the sphere

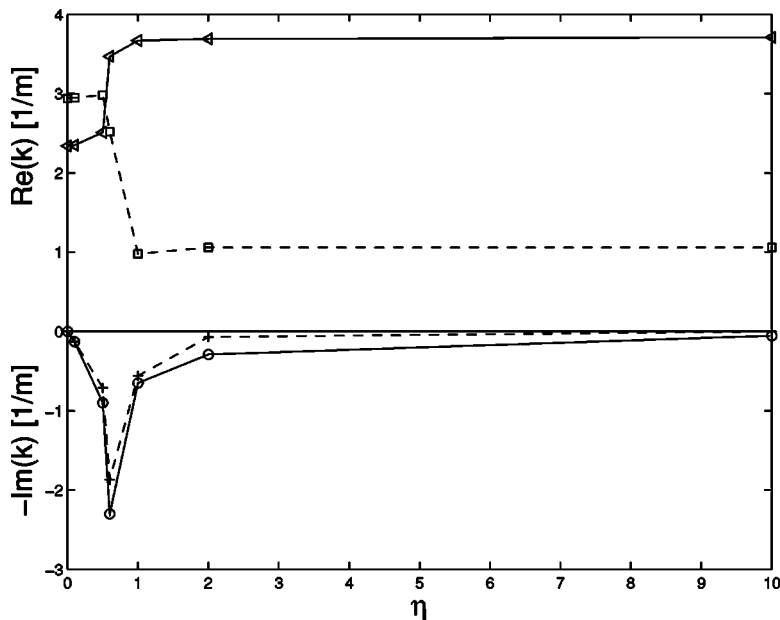


FIG. 2. The real and imaginary part of the wave number as a function of specific impedance for the  $(\rho, \sigma, \tau) = (0, 0, 0)$  (solid line) and  $(\rho, \sigma, \tau) = (1, 0, 0)$  (dashed line) modes.

problem, the first excited state would be three-fold degenerate.

### B. Modes in a triaxial ellipsoid with rigid walls

In the third row of Fig. 1, the fundamental mode is plotted along the three planes mentioned above corresponding to the case with rigid walls ( $\eta = \infty$ ), i.e.,

$$\left. \frac{\partial \Psi}{\partial n} \right|_{(\xi_1 = \xi_{1ref})} = 0, \quad (24)$$

where  $\partial \Psi / \partial n$  denotes the partial derivative along the surface normal. This solution corresponds to an eigenfrequency of 58 Hz ( $\gamma = 0.49$ ) and the indices  $n, m, \rho, \sigma, \tau$  equal to 0, 0, 1, 0, 0, respectively (the corresponding frequency for a spherical enclosure having the same volume is 79 Hz). There is another solution with a smaller eigenfrequency, namely  $f = 0$  ( $\gamma = 0$ ). However, this is the trivial solution where  $F = \text{const}$  and  $\rho = \sigma = \tau = 0$ . Since the fundamental mode has the same set of indices in  $\rho, \sigma, \tau$  as the first-excited state with pressure-release walls this eigenmode is zero in the  $z = 0$  plane [refer to Eq. (23)]. The middle and right plots of Fig. 1, third row reveal that the fundamental mode satisfies Neumann boundary conditions on the curved ellipsoid boundary side as it must.

In the fourth row of Fig. 1, the first excited state is shown. This state has an eigenfrequency of 76 Hz ( $\gamma = 0.84$ ) and is associated with indices  $n, m, \rho, \sigma, \tau$  equal to 0, 0, 0, 1, 0. The form of this eigenmode is

$$\Psi(\xi_1, \xi_2, \xi_3) = \left( \frac{\xi_1^2}{b^2} - 1 \right)^{1/2} \left( \frac{\xi_2^2}{b^2} - 1 \right)^{1/2} \left( \frac{\xi_3^2}{b^2} - 1 \right)^{1/2} \times F(\xi_1)F(\xi_2)F(\xi_3), \quad (25)$$

where, again,  $F$  is the solution to Eq. (16). Hence, this state is zero in the  $y = 0$  plane (right plot) where  $\xi_2 = b$  or  $\xi_3 = b$ . The left and middle plots (fourth row of Fig. 1) show that Neumann boundary conditions are fulfilled along the curved ellipsoid boundary side.

### C. Modes in a triaxial ellipsoid with lossy walls

Next, let us consider the general case with a finite, non-zero specific impedance such that the boundary conditions are of mixed type [Eq. (2)]. The variation in the complex wave number is plotted in Fig. 2 for the fundamental mode for  $\eta = 0$  and the corresponding first excited mode. As is commonly done in plotting complex electronic band structures, we have plotted the real (imaginary) part of the wave number along the positive (negative)  $y$  axis. This plot reveals a number of interesting results. It is evident that the calculated eigenfrequencies are real when  $\eta = 0$  and  $\eta = \infty$ , however, for a finite, nonzero specific impedance,  $\gamma$  becomes complex due to the mixed boundary condition with an imaginary coefficient. In other words, the pressure mode decays exponentially with time when the specific impedance is finite and acoustic losses take place at the ellipsoidal walls. Furthermore, there is a rapid convergence of the real part of the wave number with  $\eta$ ; indeed, the results with  $\eta = 2$  are less than 2% from the  $\eta = \infty$  results. While the real parts for the two modes shown differ significantly, the imaginary parts are quite similar. They both reach a maximum near the crossing of the real parts. The similarity in the damping constants can be understood in terms of earlier results that the damping constant is mostly influenced by the wall impedance. A possible explanation of the near coincidence of the maximum in the damping constant with the mode degeneracy is due to the correspondence of the damping constant with the linewidth of the resonance (in frequency space). Thus, if the resonance width is larger than the resonance separation, the neighboring resonances cannot be resolved and they are quasi-degenerate. We also note that the imaginary part of the wave number is usually much smaller than the real part<sup>13</sup> except near the crossing.

The fundamental mode plotted along the three planes  $z = 0$ ,  $x = 0$ , and  $y = 0$  is shown in the fifth row of Fig. 1. In general, the eigenfunction is complex and we have plotted the modulus. Since this state is characterized by  $\rho = \sigma = \tau = 0$ , this eigenmode has no nodal plane along the three Car-

tesian axes. In the sixth row of Fig. 1, the first-excited state for  $\eta=0.6$  is plotted along the three planes. As mentioned earlier, due to  $\rho=1$ , this state has a nodal plane ( $z=0$ ).

#### IV. CONCLUSION

A quasi-analytical solution of the vibrational modes in triaxial ellipsoidal cavities was obtained for the case with arbitrary acoustic impedance boundary conditions. Complex wavenumber data and eigenmode plots are given for the cases:  $\rho, \sigma, \tau$  equal to 0,0,0 and 1,0,0 being the fundamental-mode indices corresponding to pressure-release and rigid-wall boundary conditions, respectively. A mode crossing of the lowest two modes was found to occur at an intermediate specific acoustic impedance with a corresponding peak in the damping constant.

#### ACKNOWLEDGMENTS

The Work of LYV was partially supported by a NSF CAREER award (NSF Grant No. 9984059) and a Balslev award (Denmark).

- <sup>1</sup>H. Levine, "Acoustical cavity excitation," J. Acoust. Soc. Am. **109**, 2555–2565 (2001).
- <sup>2</sup>A. Ali, C. Rajakumar, and S. M. Yunus, "Advances in acoustic eigenvalue analysis using boundary element method," Comput. Struct. **56**, 837–847 (1995).
- <sup>3</sup>P. M. Morse and H. Feshbach, *Methods of Theoretical Physics* (McGraw-Hill, New York, 1953).

- <sup>4</sup>H. Lamb, *The Dynamical Theory of Sound* (Dover, New York, 1960).
- <sup>5</sup>C. T. M. Chang, "Natural resonant frequency of a prolate acoustical resonator," J. Acoust. Soc. Am. **49**, 611–614 (1971).
- <sup>6</sup>K. Hong and J. Kim, "Natural mode analysis of hollow and annular elliptical cylindrical cavities," J. Sound Vib. **183**, 327–351 (1995).
- <sup>7</sup>M. Willatzen and L. C. Lew Yan Voon, "Acoustic eigenmodes in parabolic cylindrical structures," in the *Proceedings of the Tenth International Congress on Sound and Vibration*, 7–10 July, Stockholm, Sweden, 2003, pp. 3279–3286.
- <sup>8</sup>M. Willatzen and L. C. Lew Yan Voon, "Acoustic cavity modes in lens-shaped crystals," J. Acoust. Soc. Am. **115**, 84–90 (2004).
- <sup>9</sup>J. Yan and K. K. Yen, "A derivation of three-dimensional ray equations in ellipsoidal coordinates," J. Acoust. Soc. Am. **97**, 1538–1544 (1995).
- <sup>10</sup>M. R. Bailey, D. T. Blackstock, R. O. Cleveland, and L. A. Crum, "Comparison of electrohydraulic lithotripters with rigid and pressure-release ellipsoidal reflectors. II. Cavitation fields," J. Acoust. Soc. Am. **106**, 1149–1160 (1999).
- <sup>11</sup>S. G. Conti, P. Roux, D. A. Demer, and J. de Rosny, "Measurements of the total scattering and absorption cross-sections of the human body," J. Acoust. Soc. Am. **114**, 2357 (2003).
- <sup>12</sup>R. Garmier and J.-P. Barriot, "Ellipsoidal harmonic expansions of the gravitational potential: theory and application," Celest. Mech. Dyn. Astron. **79**, 235–275 (2001).
- <sup>13</sup>P. M. Morse and K. U. Ingard, *Theoretical Acoustics* (McGraw-Hill, New York, 1968).
- <sup>14</sup>A. D. Pierce, *Acoustics: An Introduction to Its Physical Principles and Applications* (McGraw-Hill, New York, 1981).
- <sup>15</sup>P. Moon and D. E. Spencer, *Field Theory Handbook* (Springer-Verlag, Berlin, 1961).
- <sup>16</sup>G. B. Arfken, *Mathematical Methods for Physicists* (Academic, San Diego, 1966).
- <sup>17</sup>F. M. Arscott, P. J. Taylor, and R. V. M. Zahar, "On the numerical construction of ellipsoidal wave functions," in Math. Comput. **40**, 367–380 (1983).